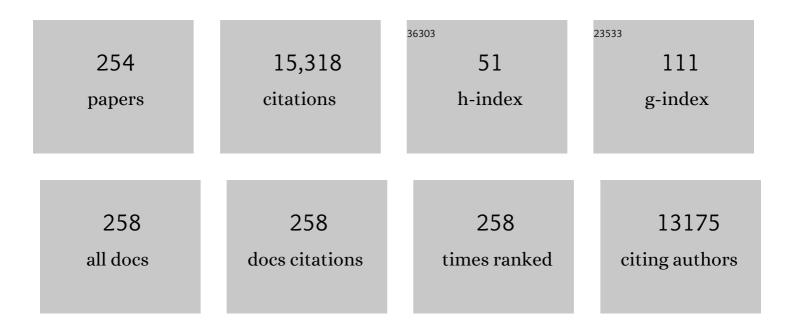


## List of Publications by Year in descending order

Source: https://exaly.com/author-pdf/8547551/publications.pdf Version: 2024-02-01



#	Article	IF	CITATIONS
1	Discovery of novel inhibitors of SARS-CoV-2 main protease. Journal of Biomolecular Structure and Dynamics, 2022, 40, 12526-12534.	3.5	2
2	Insights into small molecule inhibitor bindings to PD-L1 with residue-specific binding free energy calculation. Journal of Biomolecular Structure and Dynamics, 2022, 40, 12277-12285.	3.5	1
3	HobPre: accurate prediction of human oral bioavailability for small molecules. Journal of Cheminformatics, 2022, 14, 1.	6.1	32
4	Discovery of novel inhibitors of CDK2 using docking and physicsâ€based binding free energy calculation. Chemical Biology and Drug Design, 2022, 99, 662-673.	3.2	4
5	Computational Alanine Scanning Reveals Common Features of TCR/pMHC Recognition in HLA-DQ8-Associated Celiac Disease. Methods in Molecular Biology, 2022, 2385, 293-312.	0.9	Ο
6	<i>Ab initio</i> neural network MD simulation of thermal decomposition of a high energy material CL-20/TNT. Physical Chemistry Chemical Physics, 2022, 24, 11801-11811.	2.8	13
7	Mutational Effect of Some Major COVID-19 Variants on Binding of the S Protein to ACE2. Biomolecules, 2022, 12, 572.	4.0	8
8	HergSPred: Accurate Classification of hERG Blockers/Nonblockers with Machine-Learning Models. Journal of Chemical Information and Modeling, 2022, 62, 1830-1839.	5.4	26
9	AA-Score: a New Scoring Function Based on Amino Acid-Specific Interaction for Molecular Docking. Journal of Chemical Information and Modeling, 2022, 62, 2499-2509.	5.4	11
10	SeBPPI: A Sequence-Based Protein–Protein Binding Predictor. Journal of Computational Biophysics and Chemistry, 2022, 21, 729-737.	1.7	2
11	Rational Design of P450 aMOx for Improving Anti-Markovnikov Selectivity Based on the "Butterfly― Model. Frontiers in Molecular Biosciences, 2022, 9, .	3.5	2
12	Immune Escape Mechanisms of SARS-CoV-2 Delta and Omicron Variants against Two Monoclonal Antibodies That Received Emergency Use Authorization. Journal of Physical Chemistry Letters, 2022, 13, 6064-6073.	4.6	14
13	Molecular basis of SMAC-XIAP binding and the effect of electrostatic polarization. Journal of Biomolecular Structure and Dynamics, 2021, 39, 743-752.	3.5	7
14	Alanine scanning combined with interaction entropy studying the differences of binding mechanism on HIV-1 and HIV-2 proteases with inhibitor. Journal of Biomolecular Structure and Dynamics, 2021, 39, 1588-1599.	3.5	5
15	Identification of three new compounds that directly target human serine hydroxymethyltransferase 2. Chemical Biology and Drug Design, 2021, 97, 221-230.	3.2	6
16	Inhibition mechanism and hot-spot prediction of nine potential drugs for SARS-CoV-2 M <sup>pro</sup> by large-scale molecular dynamic simulations combined with accurate binding free energy calculations. Nanoscale, 2021, 13, 8313-8332.	5.6	8
17	A fixed multi-site interaction charge model for an accurate prediction of the QM/MM interactions. Physical Chemistry Chemical Physics, 2021, 23, 21001-21012.	2.8	1
18	Molecular mechanism related to the binding of fluorophores to Mango-II revealed by multiple-replica molecular dynamics simulations. Physical Chemistry Chemical Physics, 2021, 23, 10636-10649.	2.8	6

#	Article	IF	CITATIONS
19	Cyclopentadienyl radical formation from the reaction of excited nitrogen atoms with benzene: a theoretical study. Physical Chemistry Chemical Physics, 2021, 23, 12408-12420.	2.8	9
20	Residue-specific binding mechanisms of PD-L1 to its monoclonal antibodies by computational alanine scanning. Physical Chemistry Chemical Physics, 2021, 23, 15591-15600.	2.8	0
21	Multiscale polarizable coarse-graining water models on cluster-level electrostatic dipoles. Physical Chemistry Chemical Physics, 2021, 23, 8926-8935.	2.8	3
22	Engineering the biomimetic cofactors of NMNH for cytochrome P450 BM3 based on binding conformation refinement. RSC Advances, 2021, 11, 12036-12042.	3.6	4
23	Quantitative analysis of ACE2 binding to coronavirus spike proteins: SARS-CoV-2 <i>vs.</i> SARS-CoV and RaTG13. Physical Chemistry Chemical Physics, 2021, 23, 13926-13933.	2.8	11
24	Thermodynamic Insights of Base Flipping in TNA Duplex: Force Fields, Salt Concentrations, and Free-Energy Simulation Methods. CCS Chemistry, 2021, 3, 1026-1039.	7.8	23
25	Computational Analysis of Residue-Specific Binding Free Energies of Androgen Receptor to Ligands. Frontiers in Molecular Biosciences, 2021, 8, 646524.	3.5	5
26	An electrostatic energy-based charge model for molecular dynamics simulation. Journal of Chemical Physics, 2021, 154, 134107.	3.0	5
27	Fragment-Based Ab Initio Molecular Dynamics Simulation for Combustion. Molecules, 2021, 26, 3120.	3.8	1
28	Investigation on the characteristics and mechanisms of ACE inhibitory peptides by a thorough analysis of all 8000 tripeptides via binding free energy calculation. Food Science and Nutrition, 2021, 9, 2943-2953.	3.4	11
29	Analysis of the binding modes of the first―and secondâ€generation antiandrogens with respect to F876L mutation. Chemical Biology and Drug Design, 2021, 98, 60-72.	3.2	1
30	DeepBSP—a Machine Learning Method for Accurate Prediction of Protein–Ligand Docking Structures. Journal of Chemical Information and Modeling, 2021, 61, 2231-2240.	5.4	44
31	Automatically Constructed Neural Network Potentials for Molecular Dynamics Simulation of Zinc Proteins. Frontiers in Chemistry, 2021, 9, 692200.	3.6	10
32	Ultra-coarse-graining modeling of liquid water. Journal of Chemical Physics, 2021, 154, 224506.	3.0	3
33	Anchor-Locker Binding Mechanism of the Coronavirus Spike Protein to Human ACE2: Insights from Computational Analysis. Journal of Chemical Information and Modeling, 2021, 61, 3529-3542.	5.4	26
34	MolGpka: A Web Server for Small Molecule p <i>K</i> <sub>a</sub> Prediction Using a Graph-Convolutional Neural Network. Journal of Chemical Information and Modeling, 2021, 61, 3159-3165.	5.4	79
35	Investigating effects of bridging water on the binding of neuraminidaseâ^'ligands using computational alanine scanning combined with interaction entropy method. Journal of Molecular Liquids, 2021, 336, 116214.	4.9	1
36	Rational Design of Pepsin for Enhanced Thermostability via Exploiting the Guide of Structural Weakness on Stability. Frontiers in Physics, 2021, 9, .	2.1	5

#	Article	IF	CITATIONS
37	CHARMM-GUI Supports Hydrogen Mass Repartitioning and Different Protonation States of Phosphates in Lipopolysaccharides. Journal of Chemical Information and Modeling, 2021, 61, 831-839.	5.4	59
38	Computational analysis of binding free energies, hotspots and the binding mechanism of Bcl-xL/Bcl-2 binding to Bad/Bax. Physical Chemistry Chemical Physics, 2021, 23, 2025-2037.	2.8	6
39	Introducing the effective polarizable bond (EPB) model in DNA simulations. Chemical Physics Letters, 2021, 785, 139160.	2.6	0
40	Computational Insights into the Binding Mechanism of OxyS sRNA with Chaperone Protein Hfq. Biomolecules, 2021, 11, 1653.	4.0	1
41	Automated Construction of Neural Network Potential Energy Surface: The Enhanced Self-Organizing Incremental Neural Network Deep Potential Method. Journal of Chemical Information and Modeling, 2021, 61, 5425-5437.	5.4	6
42	Targeting mechanism for SARS-CoV-2 <i>in silico</i> : interaction and key groups of TMPRSS2 toward four potential drugs. Nanoscale, 2021, 13, 19218-19237.	5.6	2
43	Binding modes and conformational changes of FK506-binding protein 51 induced by inhibitor bindings: insight into molecular mechanisms based on multiple simulation technologies. Journal of Biomolecular Structure and Dynamics, 2020, 38, 2141-2155.	3.5	16
44	Decoding molecular mechanism of inhibitor bindings to CDK2 using molecular dynamics simulations and binding free energy calculations. Journal of Biomolecular Structure and Dynamics, 2020, 38, 985-996.	3.5	29
45	CHARMMâ€GUI DEER facilitator for spinâ€pair distance distribution calculations and preparation of restrainedâ€ensemble molecular dynamics simulations. Journal of Computational Chemistry, 2020, 41, 415-420.	3.3	19
46	LLPSDB: a database of proteins undergoing liquid–liquid phase separation in vitro. Nucleic Acids Research, 2020, 48, D320-D327.	14.5	130
47	Determining Optimal Coarseâ€Grained Representation for Biomolecules Using Internal Cluster Validation Indexes. Journal of Computational Chemistry, 2020, 41, 14-20.	3.3	9
48	Theoretical understanding of the thermodynamics and interactions in transcriptional regulator TtgR–ligand binding. Physical Chemistry Chemical Physics, 2020, 22, 1511-1524.	2.8	13
49	Binding Modes of Smallâ€Molecule Inhibitors to the EED Pocket of PRC2. ChemPhysChem, 2020, 21, 263-271.	2.1	11
50	Development of a New Scoring Function for Virtual Screening: APBScore. Journal of Chemical Information and Modeling, 2020, 60, 6355-6365.	5.4	11
51	Complex reaction processes in combustion unraveled by neural network-based molecular dynamics simulation. Nature Communications, 2020, 11, 5713.	12.8	111
52	A three-point coarse-grained model of five-water cluster with permanent dipoles and quadrupoles. Physical Chemistry Chemical Physics, 2020, 22, 26289-26298.	2.8	2
53	Double-Well Ultra-Coarse-Grained Model to Describe Protein Conformational Transitions. Journal of Chemical Theory and Computation, 2020, 16, 6678-6689.	5.3	20
54	An Approach to Computing Solvent Reorganization Energy. Journal of Chemical Theory and Computation, 2020, 16, 6513-6519.	5.3	3

#	Article	IF	CITATIONS
55	An ab initio/RRKM study of the reaction mechanism and product branching ratios of CH3OH+ and CH3OH++ dissociation. Journal of Molecular Structure, 2020, 1217, 128410.	3.6	4
56	DenseCPD: Improving the Accuracy of Neural-Network-Based Computational Protein Sequence Design with DenseNet. Journal of Chemical Information and Modeling, 2020, 60, 1245-1252.	5.4	47
57	Computational approaches to studying methylated H4K20 recognition by DNA repair factor 53BP1. Physical Chemistry Chemical Physics, 2020, 22, 6136-6144.	2.8	11
58	Entropic effect and residue specific entropic contribution to the cooperativity in streptavidin–biotin binding. Nanoscale, 2020, 12, 7134-7145.	5.6	21
59	How CuCl and CuCl <sub>2</sub> Insert into C–N Bonds of Diazo Compounds: An Electronic Structure and Mechanistic Study. Journal of Physical Chemistry A, 2020, 124, 2029-2035.	2.5	5
60	Atomic-level reconstruction of biomolecules by a rigid-fragment- and local-frame-based (RF-LF) strategy. Journal of Molecular Modeling, 2020, 26, 31.	1.8	3
61	Molecular Mechanism of Selective Binding of NMS-P118 to PARP-1 and PARP-2: A Computational Perspective. Frontiers in Molecular Biosciences, 2020, 7, 50.	3.5	13
62	Developing an effective polarizable bond method for small molecules with application to optimized molecular docking. RSC Advances, 2020, 10, 15530-15540.	3.6	14
63	An Energy Optimization Strategy Based on the Perfect Conformation of Prolyl Endopeptidase for Improving Catalytic Efficiency. Journal of Agricultural and Food Chemistry, 2020, 68, 5129-5137.	5.2	8
64	An accurate free energy estimator: based on MM/PBSA combined with interaction entropy for protein–ligand binding affinity. Nanoscale, 2020, 12, 10737-10750.	5.6	88
65	A method for efficient calculation of thermal stability of proteins upon point mutations. Physical Chemistry Chemical Physics, 2020, 22, 8461-8466.	2.8	12
66	Accelerated Molecular Dynamics Simulation for Helical Proteins Folding in Explicit Water. Frontiers in Chemistry, 2019, 7, 540.	3.6	56
67	Molecular Dynamics Simulation of Zinc Ion in Water with an ab Initio Based Neural Network Potential. Journal of Physical Chemistry A, 2019, 123, 6587-6595.	2.5	24
68	A Fragment Quantum Mechanical Method for Metalloproteins. Journal of Chemical Theory and Computation, 2019, 15, 1430-1439.	5.3	17
69	Study of SHMT2 Inhibitors and Their Binding Mechanism by Computational Alanine Scanning. Journal of Chemical Information and Modeling, 2019, 59, 3871-3878.	5.4	21
70	Computational analysis for residue-specific CDK2-inhibitor bindings. Chinese Journal of Chemical Physics, 2019, 32, 134-142.	1.3	10
71	Mechanistic Studies of CO2 Cycloaddition Reaction Catalyzed by Amine-Functionalized Ionic Liquids. Frontiers in Chemistry, 2019, 7, 615.	3.6	20
72	Drug-resistance mechanisms of three mutations in anaplastic lymphoma kinase against two inhibitors based on MM/PBSA combined with interaction entropy. Physical Chemistry Chemical Physics, 2019, 21, 20951-20964.	2.8	9

#	Article	IF	CITATIONS
73	A force consistent method for electrostatic energy calculation in fluctuating charge model. Journal of Chemical Physics, 2019, 151, 094105.	3.0	3
74	CHARMM-GUI <i>Glycan Modeler</i> for modeling and simulation of carbohydrates and glycoconjugates. Glycobiology, 2019, 29, 320-331.	2.5	222
75	CHARMMâ€GUI <i>Nanodisc Builder</i> for modeling and simulation of various nanodisc systems. Journal of Computational Chemistry, 2019, 40, 893-899.	3.3	42
76	End-Point Binding Free Energy Calculation with MM/PBSA and MM/GBSA: Strategies and Applications in Drug Design. Chemical Reviews, 2019, 119, 9478-9508.	47.7	1,064
77	Sulfur-substitution-induced base flipping in the DNA duplex. Physical Chemistry Chemical Physics, 2019, 21, 14923-14940.	2.8	21
78	Effect of mutations on binding of ligands to guanine riboswitch probed by free energy perturbation and molecular dynamics simulations. Nucleic Acids Research, 2019, 47, 6618-6631.	14.5	130
79	Computational analysis of hot spots and binding mechanism in the PD-1/PD-L1 interaction. RSC Advances, 2019, 9, 14944-14956.	3.6	23
80	BARâ€based optimum adaptive steered MD for configurational sampling. Journal of Computational Chemistry, 2019, 40, 1270-1289.	3.3	22
81	DeepDDG: Predicting the Stability Change of Protein Point Mutations Using Neural Networks. Journal of Chemical Information and Modeling, 2019, 59, 1508-1514.	5.4	146
82	Understanding the selectivity of inhibitors toward PI4KIIIα and PI4KIIIβ based molecular modeling. Physical Chemistry Chemical Physics, 2019, 21, 22103-22112.	2.8	22
83	Formation mechanism and spectroscopy of C <sub>6</sub> H radicals in extreme environments: a theoretical study. Physical Chemistry Chemical Physics, 2019, 21, 23044-23055.	2.8	5
84	Accurate and Efficient Calculation of Protein–Protein Binding Free Energy-Interaction Entropy with Residue Type-Specific Dielectric Constants. Journal of Chemical Information and Modeling, 2019, 59, 272-281.	5.4	37
85	Calculation of hot spots for protein–protein interaction in p53/PMIâ€MDM2/MDMX complexes. Journal of Computational Chemistry, 2019, 40, 1045-1056.	3.3	22
86	CHARMM-GUI <i>Membrane Builder</i> for Complex Biological Membrane Simulations with Glycolipids and Lipoglycans. Journal of Chemical Theory and Computation, 2019, 15, 775-786.	5.3	388
87	An efficient method for computing excess free energy of liquid. Science China Chemistry, 2018, 61, 135-140.	8.2	20
88	Computational Protein Design with Deep Learning Neural Networks. Scientific Reports, 2018, 8, 6349.	3.3	112
89	Computational Alanine Scanning with Interaction Entropy for Protein–Ligand Binding Free Energies. Journal of Chemical Theory and Computation, 2018, 14, 1772-1780.	5.3	78
90	Multiple Conformational States Contribute to the 3D Structure of a Glucan Decasaccharide: A Combined SAXS and MD Simulation Study. Journal of Physical Chemistry B, 2018, 122, 1169-1175.	2.6	9

#	Article	IF	CITATIONS
91	A Coupled Ionization-Conformational Equilibrium Is Required To Understand the Properties of Ionizable Residues in the Hydrophobic Interior of Staphylococcal Nuclease. Journal of the American Chemical Society, 2018, 140, 1639-1648.	13.7	22
92	Crius: A novel fragmentâ€based algorithm of <i>de novo</i> substrate prediction for enzymes. Protein Science, 2018, 27, 1526-1534.	7.6	0
93	Assessing the performance of MM/PBSA and MM/GBSA methods. 7. Entropy effects on the performance of end-point binding free energy calculation approaches. Physical Chemistry Chemical Physics, 2018, 20, 14450-14460.	2.8	243
94	Unfolding of a CIC chloride transporter retains memory of its evolutionary history. Nature Chemical Biology, 2018, 14, 489-496.	8.0	39
95	Interaction entropy for computational alanine scanning in protein-protein binding. Wiley Interdisciplinary Reviews: Computational Molecular Science, 2018, 8, e1342.	14.6	51
96	Hydrogen-bond structure dynamics in bulk water: insights from <i>ab initio</i> simulations with coupled cluster theory. Chemical Science, 2018, 9, 2065-2073.	7.4	98
97	The impact of interior dielectric constant and entropic change on HIV-1 complex binding free energy prediction. Structural Dynamics, 2018, 5, 064101.	2.3	44
98	Effect of Substituents in Different Positions of Aminothiazole Hinge-Binding Scaffolds on Inhibitor–CDK2 Association Probed by Interaction Entropy Method. ACS Omega, 2018, 3, 18052-18064.	3.5	18
99	Probing the Ion-Specific Effects at the Water/Air Interface and Water-Mediated Ion Pairing in Sodium Halide Solution with <i>Ab Initio</i> Molecular Dynamics. Journal of Physical Chemistry B, 2018, 122, 10202-10209.	2.6	19
100	Exploring the Reasons for Decrease in Binding Affinity of HIV-2 Against HIV-1 Protease Complex Using Interaction Entropy Under Polarized Force Field. Frontiers in Chemistry, 2018, 6, 380.	3.6	14
101	Functional loop dynamics of the S-component of ECF transporter FolT. Molecular Physics, 2018, 116, 2613-2621.	1.7	0
102	Electrostatic Polarization Effect on Cooperative Aggregation of Full Length Human Islet Amyloid. Journal of Chemical Information and Modeling, 2018, 58, 1587-1595.	5.4	2
103	Automated Fragmentation QM/MM Calculation of NMR Chemical Shifts for Protein-Ligand Complexes. Frontiers in Chemistry, 2018, 6, 150.	3.6	14
104	A Force Balanced Fragmentation Method for ab Initio Molecular Dynamic Simulation of Protein. Frontiers in Chemistry, 2018, 6, 189.	3.6	5
105	Residue-specific free energy analysis in ligand bindings to JAK2. Molecular Physics, 2018, 116, 2633-2641.	1.7	16
106	Evaluation of the Coupled Two-Dimensional Main Chain Torsional Potential in Modeling Intrinsically Disordered Proteins. Journal of Chemical Information and Modeling, 2017, 57, 267-274.	5.4	6
107	Performance Comparison of Systematic Methods for Rigorous Definition of Coarse-Grained Sites of Large Biomolecules. Journal of Chemical Information and Modeling, 2017, 57, 214-222.	5.4	6
108	Protein simulation using coarse-grained two-bead multipole force field with polarizable water models. Journal of Chemical Physics, 2017, 146, 065101.	3.0	3

#	Article	IF	CITATIONS
109	Effect of polarization on HIV-1protease and fluoro-substituted inhibitors binding energies by large scale molecular dynamics simulations. Scientific Reports, 2017, 7, 42223.	3.3	20
110	Two-bead polarizable water models combined with a two-bead multipole force field (TMFF) for coarse-grained simulation of proteins. Physical Chemistry Chemical Physics, 2017, 19, 7410-7419.	2.8	9
111	Modeling and simulation of bacterial outer membranes and interactions with membrane proteins. Current Opinion in Structural Biology, 2017, 43, 131-140.	5.7	42
112	Interaction Entropy for Computational Alanine Scanning. Journal of Chemical Information and Modeling, 2017, 57, 1112-1122.	5.4	80
113	Fragment Quantum Mechanical Method for Large-Sized Ion–Water Clusters. Journal of Chemical Theory and Computation, 2017, 13, 2021-2034.	5.3	54
114	Direct folding simulation of helical proteins using an effective polarizable bond force field. Physical Chemistry Chemical Physics, 2017, 19, 15273-15284.	2.8	13
115	An Electrochemical Biosensor with Dual Signal Outputs: Toward Simultaneous Quantification of pH and O <sub>2</sub> in the Brain upon Ischemia and in a Tumor during Cancer Starvation Therapy. Angewandte Chemie - International Edition, 2017, 56, 10471-10475.	13.8	84
116	Single Biosensor for Simultaneous Quantification of Glucose and pH in a Rat Brain of Diabetic Model Using Both Current and Potential Outputs. Analytical Chemistry, 2017, 89, 6656-6662.	6.5	45
117	Interaction entropy for protein-protein binding. Journal of Chemical Physics, 2017, 146, 124124.	3.0	92
118	Full QM Calculation of RNA Energy Using Electrostatically Embedded Generalized Molecular Fractionation with Conjugate Caps Method. Journal of Physical Chemistry A, 2017, 121, 2503-2514.	2.5	21
119	CHARMM-GUI MDFF/xMDFF Utilizer for Molecular Dynamics Flexible Fitting Simulations in Various Environments. Journal of Physical Chemistry B, 2017, 121, 3718-3723.	2.6	24
120	CHARMMâ€GUI Martini Maker for modeling and simulation of complex bacterial membranes with lipopolysaccharides. Journal of Computational Chemistry, 2017, 38, 2354-2363.	3.3	150
121	Origins of Protons in C–H Bond Insertion Products of Phenols: Proton-Self-Sufficient Function via Water Molecules. Journal of Physical Chemistry A, 2017, 121, 6523-6529.	2.5	8
122	A theoretical study of the substituent effect on reactions of amines, carbon dioxide and ethylene oxide catalyzed by binary ionic liquids. RSC Advances, 2017, 7, 51521-51527.	3.6	11
123	An Electrochemical Biosensor with Dual Signal Outputs: Toward Simultaneous Quantification of pH and O <sub>2</sub> in the Brain upon Ischemia and in a Tumor during Cancer Starvation Therapy. Angewandte Chemie, 2017, 129, 10607-10611.	2.0	19
124	Protein–Ligand Empirical Interaction Components for Virtual Screening. Journal of Chemical Information and Modeling, 2017, 57, 1793-1806.	5.4	51
125	CHARMMâ€GUI 10 years for biomolecular modeling and simulation. Journal of Computational Chemistry, 2017, 38, 1114-1124.	3.3	224
126	<i>Ab initio</i> Quantum Mechanics/Molecular Mechanics Molecular Dynamics Simulation of CO in the Heme Distal Pocket of Myoglobin. Chinese Journal of Chemical Physics, 2017, 30, 705-716.	1.3	5

#	Article	IF	CITATIONS
127	Asymmetric Cryo-EM Structure of Anthrax Toxin Protective Antigen Pore with Lethal Factor N-Terminal Domain. Toxins, 2017, 9, 298.	3.4	12
128	Computational Study of PCSK9-EGFA Complex with Effective Polarizable Bond Force Field. Frontiers in Molecular Biosciences, 2017, 4, 101.	3.5	3
129	Preferred conformations of <i>N</i> -glycan core pentasaccharide in solution and in glycoproteins. Glycobiology, 2016, 26, cwv083.	2.5	34
130	A new algorithm for construction of coarse-grained sites of large biomolecules. Journal of Computational Chemistry, 2016, 37, 795-804.	3.3	18
131	A systematic study on RNA NMR chemical shift calculation based on the automated fragmentation QM/MM approach. RSC Advances, 2016, 6, 108590-108602.	3.6	14
132	Conformational Flexibility of a Short Loop near the Active Site of the SARS-3CLpro is Essential to Maintain Catalytic Activity. Scientific Reports, 2016, 6, 20918.	3.3	20
133	Constructing Optimal Coarse-Grained Sites of Huge Biomolecules by Fluctuation Maximization. Journal of Chemical Theory and Computation, 2016, 12, 2091-2100.	5.3	19
134	Interaction Entropy: A New Paradigm for Highly Efficient and Reliable Computation of Protein–Ligand Binding Free Energy. Journal of the American Chemical Society, 2016, 138, 5722-5728.	13.7	297
135	Replacing Arginine 33 for Alanine in the Hemophore HasA from <i>Pseudomonas aeruginosa</i> Causes Closure of the H32 Loop in the Apo-Protein. Biochemistry, 2016, 55, 2622-2631.	2.5	12
136	PBSA_E: A PBSA-Based Free Energy Estimator for Protein–Ligand Binding Affinity. Journal of Chemical Information and Modeling, 2016, 56, 854-861.	5.4	12
137	Effects of Spin-Labels on Membrane Burial Depth of MARCKS-ED Residues. Biophysical Journal, 2016, 111, 1600-1603.	0.5	0
138	DFT Calculations on the Mechanism of Transition-Metal-Catalyzed Reaction of Diazo Compounds with Phenols: O–H Insertion versus C–H Insertion. Journal of Physical Chemistry A, 2016, 120, 6485-6492.	2.5	45
139	A Semiautomated Structure-Based Method To Predict Substrates of Enzymes via Molecular Docking: A Case Study with <i>Candida antarctica</i> Lipase B. Journal of Chemical Information and Modeling, 2016, 56, 1979-1994.	5.4	5
140	The origin of the cooperativity in the streptavidin-biotin system: A computational investigation through molecular dynamics simulations. Scientific Reports, 2016, 6, 27190.	3.3	28
141	Examination of the quality of various force fields and solvation models for the equilibrium simulations of GA88 and GB88. Journal of Molecular Modeling, 2016, 22, 177.	1.8	5
142	TMFF—A Two-Bead Multipole Force Field for Coarse-Grained Molecular Dynamics Simulation of Protein. Journal of Chemical Theory and Computation, 2016, 12, 6147-6156.	5.3	12
143	BamA POTRA Domain Interacts with a Native Lipid Membrane Surface. Biophysical Journal, 2016, 110, 2698-2709.	0.5	65
144	The effect of POPC acyl chains packing by aromatic amino acid methyl esters investigated by ATR-FTIR combined with QM calculations. RSC Advances, 2016, 6, 45569-45577.	3.6	7

#	Article	IF	CITATIONS
145	Calculations of Solvation Free Energy through Energy Reweighting from Molecular Mechanics to Quantum Mechanics. Journal of Chemical Theory and Computation, 2016, 12, 499-511.	5.3	78
146	CHARMM-GUI Input Generator for NAMD, GROMACS, AMBER, OpenMM, and CHARMM/OpenMM Simulations Using the CHARMM36 Additive Force Field. Journal of Chemical Theory and Computation, 2016, 12, 405-413.	5.3	2,567
147	Dynamics and Interactions of OmpF and LPS: Influence on Pore Accessibility and Ion Permeability. Biophysical Journal, 2016, 110, 930-938.	0.5	64
148	Mechanistic Investigation of Aromatic C(sp <sup>2</sup> )–H and Alkyl C(sp <sup>3</sup> )–H Bond Insertion by Gold Carbenes. Journal of Physical Chemistry A, 2016, 120, 1925-1932.	2.5	29
149	Hybrid QM/MM study of FMO complex with polarized protein-specific charge. Scientific Reports, 2015, 5, 17096.	3.3	30
150	Quantum mechanical calculation of electric fields and vibrational Stark shifts at active site of human aldose reductase. Journal of Chemical Physics, 2015, 143, 184111.	3.0	11
151	Roles of glycans in interactions between gp120 and HIV broadly neutralizing antibodies. Glycobiology, 2015, 26, cwv101.	2.5	15
152	Calculation of protein–ligand binding affinities based on a fragment quantum mechanical method. RSC Advances, 2015, 5, 107020-107030.	3.6	47
153	Glycosylation Modulates Human CD2-CD58 Adhesion via Conformational Adjustment. Journal of Physical Chemistry B, 2015, 119, 6493-6501.	2.6	13
154	Functional Loop Dynamics of the Streptavidin-Biotin Complex. Scientific Reports, 2015, 5, 7906.	3.3	15
155	Correct folding of an α-helix and a β-hairpin using a polarized 2D torsional potential. Scientific Reports, 2015, 5, 10359.	3.3	15
156	Solid-State NMR-Restrained Ensemble Dynamics of a Membrane Protein in Explicit Membranes. Biophysical Journal, 2015, 108, 1954-1962.	0.5	11
157	Effects of N-glycosylation on protein conformation and dynamics: Protein Data Bank analysis and molecular dynamics simulation study. Scientific Reports, 2015, 5, 8926.	3.3	187
158	Quantum Fragment Based <i>ab Initio</i> Molecular Dynamics for Proteins. Journal of Chemical Theory and Computation, 2015, 11, 5897-5905.	5.3	59
159	CHARMM-GUI Martini Maker for Coarse-Grained Simulations with the Martini Force Field. Journal of Chemical Theory and Computation, 2015, 11, 4486-4494.	5.3	340
160	CHARMM-GUI HMMM Builder for Membrane Simulations with the Highly Mobile Membrane-Mimetic Model. Biophysical Journal, 2015, 109, 2012-2022.	0.5	89
161	Insight into Early-Stage Unfolding of GPI-Anchored Human Prion Protein. Biophysical Journal, 2015, 109, 2090-2100.	0.5	18
162	Allosteric sites can be identified based on the residue-residue interaction energy difference. Proteins: Structure, Function and Bioinformatics, 2015, 83, 1375-1384.	2.6	17

#	Article	IF	CITATIONS
163	Energetics of protein backbone hydrogen bonds and their local electrostatic environment. Science China Chemistry, 2014, 57, 1708-1715.	8.2	7
164	STâ€analyzer: A webâ€based user interface for simulation trajectory analysis. Journal of Computational Chemistry, 2014, 35, 957-963.	3.3	12
165	CHARMM-GUI <i>Membrane Builder</i> toward realistic biological membrane simulations. Journal of Computational Chemistry, 2014, 35, 1997-2004.	3.3	1,802
166	CHARMM-GUI PDB Manipulator for Advanced Modeling and Simulations of Proteins Containing Nonstandard Residues. Advances in Protein Chemistry and Structural Biology, 2014, 96, 235-265.	2.3	214
167	Preferred Orientations of Phosphoinositides in Bilayers and Their Implications in Protein Recognition Mechanisms. Journal of Physical Chemistry B, 2014, 118, 4315-4325.	2.6	38
168	CHARMM-GUI PACE CG Builder for Solution, Micelle, and Bilayer Coarse-Grained Simulations. Journal of Chemical Information and Modeling, 2014, 54, 1003-1009.	5.4	47
169	Discovery of Novel Allosteric Effectors Based on the Predicted Allosteric Sites for Escherichia coli D-3-Phosphoglycerate Dehydrogenase. PLoS ONE, 2014, 9, e94829.	2.5	26
170	Interaction specific binding hotspots in Endonuclease colicin-immunity protein complex from MD simulations. Science China Chemistry, 2013, 56, 1143-1151.	8.2	7
171	Assessing the accuracy of the general AMBER force field for 2,2,2-trifluoroethanol as solvent. Journal of Molecular Modeling, 2013, 19, 2355-2361.	1.8	7
172	A New Quantum Calibrated Force Field for Zinc–Protein Complex. Journal of Chemical Theory and Computation, 2013, 9, 1788-1798.	5.3	44
173	Molecular dynamics study of DNA binding by INTâ€ĐBD under a polarized force field. Journal of Computational Chemistry, 2013, 34, 1136-1142.	3.3	5
174	A numerically stable restrained electrostatic potential charge fitting method. Journal of Computational Chemistry, 2013, 34, 847-853.	3.3	42
175	Automated Fragmentation QM/MM Calculation of Amide Proton Chemical Shifts in Proteins with Explicit Solvent Model. Journal of Chemical Theory and Computation, 2013, 9, 2104-2114.	5.3	73
176	Development of an Effective Polarizable Bond Method for Biomolecular Simulation. Journal of Physical Chemistry B, 2013, 117, 14885-14893.	2.6	19
177	Quantification of Drive-Response Relationships Between Residues During Protein Folding. Journal of Chemical Theory and Computation, 2013, 9, 3799-3805.	5.3	12
178	Direct folding simulation of a long helix in explicit water. Applied Physics Letters, 2013, 102, .	3.3	11
179	Unveiling the gating mechanism of ECF Transporter RibU. Scientific Reports, 2013, 3, 3566.	3.3	11
180	Sequence Preference of α-Helix N-Terminal Tetrapeptide. Protein and Peptide Letters, 2012, 19, 345-352.	0.9	1

#	Article	IF	CITATIONS
181	Studying the Effect of Site-Specific Hydrophobicity and Polarization on Hydrogen Bond Energy of Protein Using a Polarizable Method. Journal of Chemical Theory and Computation, 2012, 8, 2157-2164.	5.3	21
182	Identifying Allosteric Binding Sites in Proteins with a Two-State Gol Model for Novel Allosteric Effector Discovery. Journal of Chemical Theory and Computation, 2012, 8, 2962-2971.	5.3	46
183	Protein–water hydrogen bonds are stabilized by electrostatic polarization. Molecular Physics, 2012, 110, 595-604.	1.7	5
184	Effect of interprotein polarization on protein–protein binding energy. Journal of Computational Chemistry, 2012, 33, 1416-1420.	3.3	19
185	Folding and thermodynamic studies of Trp-cage based on polarized force field. Theoretical Chemistry Accounts, 2012, 131, 1.	1.4	11
186	Folding of EK peptide and its dependence on salt concentration and pH: A computational study. Science China Chemistry, 2011, 54, 1974-1981.	8.2	8
187	Computational Characterization of Binding of Small Molecule Inhibitors to HIVâ€1 gp41. Chinese Journal of Chemistry, 2011, 29, 1307-1311.	4.9	1
188	Simulation of the thermodynamics of folding and unfolding of the Trp-cage mini-protein TC5b using different combinations of force fields and solvation models. Science China Chemistry, 2010, 53, 196-201.	8.2	18
189	Maturation Mechanism of Severe Acute Respiratory Syndrome (SARS) Coronavirus 3C-like Proteinase. Journal of Biological Chemistry, 2010, 285, 28134-28140.	3.4	50
190	Folding Simulations of a De Novo Designed Protein with a βαβ Fold. Biophysical Journal, 2010, 98, 321-329.	0.5	13
191	NUMERICAL STABILITIES IN FITTING ATOMIC CHARGES TO ELECTRIC FIELD AND ELECTROSTATIC POTENTIAL. Journal of Theoretical and Computational Chemistry, 2009, 08, 925-942.	1.8	3
192	Electronic Polarization Is Important in Stabilizing the Native Structures of Proteins. Journal of Physical Chemistry B, 2009, 113, 16059-16064.	2.6	37
193	Developing Polarized Protein-Specific Charges for Protein Dynamics: MD Free Energy Calculation of pKa Shifts for Asp26/Asp20 in Thioredoxin. Biophysical Journal, 2008, 95, 1080-1088.	0.5	151
194	DESIGN OF HYBRID INHIBITORS TO HIV-1 PROTEASE. Journal of Theoretical and Computational Chemistry, 2008, 07, 485-503.	1.8	4
195	Full quantum mechanical study of binding of HIV-1 protease drugs. International Journal of Quantum Chemistry, 2005, 103, 246-257.	2.0	26
196	Quantum computational analysis for drug resistance of HIV-1 reverse transcriptase to nevirapine through point mutations. Proteins: Structure, Function and Bioinformatics, 2005, 61, 423-432.	2.6	52
197	PHOTODISSOCIATION OF OZONE IN THE HARTLEY BAND: FRAGMENT ROTATIONAL QUANTUM STATE DISTRIBUTIONS. Journal of Theoretical and Computational Chemistry, 2004, 03, 443-449.	1.8	10
198	New Advance in Computational Chemistry:  Full Quantum Mechanical ab Initio Computation of Streptavidinâ^'Biotin Interaction Energy. Journal of Physical Chemistry B, 2003, 107, 12039-12041.	2.6	117

#	Article	IF	CITATIONS
199	A mixed quantum-classical semirigid vibrating rotor target approach to methane dissociation on Ni surface. Journal of Chemical Physics, 2003, 118, 8954-8959.	3.0	27
200	Accurate quantum mechanical calculation for the N+OH reaction. Journal of Chemical Physics, 2003, 118, 6852-6857.	3.0	27
201	MIXED QUANTUM-CLASSICAL SEMI-RIGID VIBRATING ROTOR TARGET MODEL FOR ATOM-POLYATOM REACTION: O(3P) + CH4 â†' CH3 + OH. Journal of Theoretical and Computational Chemistry, 2003, 02, 351-356.	1.8	0
202	QUANTITATIVE QUANTUM DYNAMICS CALCULATION OF H2 + CH3 → H + CH4 REACTION. Journal of Theoretical and Computational Chemistry, 2002, 01, 25-29.	1.8	6
203	SVRT calculation for bond-selective reaction H+HOD→H2+OD,â€,HD+OH. Journal of Chemical Physics, 2002, 116, 10197-10200.	3.0	11
204	Application of Semirigid Vibrating Rotor Target Model to the Reaction of O(3P) + CH4→ CH3+ OHâ€. Journal of Physical Chemistry A, 2001, 105, 2530-2534.	2.5	41
205	Time-dependent wave packet calculation for state-to-state reaction of Cl+H2 using the reactant-product decoupling approach. Journal of Chemical Physics, 2001, 115, 8455-8459.	3.0	10
206	Time-dependent quantum wave packet study of the C+CH reaction. Journal of Chemical Physics, 2001, 115, 731-738.	3.0	27
207	Quantum wavepacket approach to chemical reaction dynamics. Perspective on "Dynamics of the collinear H + H 2 reaction. I. Probability density and flux". Theoretical Chemistry Accounts, 2000, 103, 300-305.	1.4	1
208	Quantum dynamics study of the Cl+D2 reaction: Time-dependent wave packet calculations. Journal of Chemical Physics, 2000, 113, 7182-7187.	3.0	27
209	Time-dependent quantum dynamics study of the Cl+H2 reaction. Journal of Chemical Physics, 2000, 113, 1434-1440.	3.0	60
210	Time-dependent quantum wave packet studies of the F+HCl and F+DCl reactions. Journal of Chemical Physics, 2000, 113, 10105-10113.	3.0	52
211	Time-Dependent Quantum Dynamics Study of the Cl + HD Reactionâ€. Journal of Physical Chemistry A, 2000, 104, 10517-10525.	2.5	20
212	Arrangement transformation approach to state-to-state quantum reactive scattering H + DH→DH + H, HH + D. Science in China Series A: Mathematics, 1999, 42, 973-979.	0.5	0
213	Six-dimensional quantum calculations of vibration-rotation-tunneling levels of $\hat{1}/21$ and $\hat{1}/22$ HCl-stretching excited (HCl)2. Journal of Chemical Physics, 1998, 108, 4804-4816.	3.0	66
214	Correction of repulsive potential energy surface for photodissociation of H2O in the $\tilde{A}f$ state. Journal of Chemical Physics, 1998, 108, 10027-10032.	3.0	3
215	Use of negative complex potential as absorbing potential. Journal of Chemical Physics, 1998, 108, 1429-1433.	3.0	52
216	Reactant-product decoupling method for state-to-state reactive scattering: A case study for 3D H+H2 exchange reaction (J=0). Journal of Chemical Physics, 1997, 106, 1742-1748.	3.0	49

#	Article	IF	CITATIONS
217	Development of Accurate Quantum Dynamical Methods for Tetraatomic Reactions. Journal of Physical Chemistry A, 1997, 101, 2746-2754.	2.5	128
218	Quantum dynamics study for reaction of H2 + OD→H + HOD. Science Bulletin, 1997, 42, 116-120.	1.7	0
219	Three-dimensional quantum dynamics study of vibrational predissociation of Hel2 van der Waals molecule for low vibrational excitation using the time-dependent wave packet method. Science in China Series B: Chemistry, 1997, 40, 442-447.	0.8	0
220	Quantum dynamics study of Li + HF reaction. Theoretical Chemistry Accounts, 1997, 96, 31-38.	1.4	44
221	Time-Dependent Wave Packet Approach to State-to-State Reactive Scattering and Application to H + O2Reaction. The Journal of Physical Chemistry, 1996, 100, 6898-6903.	2.9	111
222	Timeâ€dependent spectral calculation of bound and resonance energies of HO2. Journal of Chemical Physics, 1996, 104, 3664-3671.	3.0	40
223	Quantum mechanical tunneling through a timeâ€dependent barrier. Journal of Chemical Physics, 1996, 105, 8628-8632.	3.0	19
224	A reactantâ€product decoupling method for stateâ€ŧoâ€state reactive scattering. Journal of Chemical Physics, 1996, 105, 6072-6074.	3.0	114
225	Dissociative Adsorption of O2on Cu(110) and Cu(100):Â Three-Dimensional Quantum Dynamics Studies. The Journal of Physical Chemistry, 1996, 100, 11432-11437.	2.9	18
226	Energy Dependence of State-to-State Reaction Probabilities for H2+ OH → H + H2O in Six Dimensions. The Journal of Physical Chemistry, 1996, 100, 13901-13903.	2.9	26
227	Quantum adsorption dynamics of a diatomic molecule on surface: Fourâ€dimensional fixedâ€site model for H2 on Cu(111). Journal of Chemical Physics, 1995, 102, 6280-6289.	3.0	117
228	6D quantum calculation of energy levels for HF stretching excited (HF)2. Journal of Chemical Physics, 1995, 103, 2548-2554.	3.0	42
229	Exact fullâ€dimensional bound state calculations for (HF)2, (DF)2, and HFDF. Journal of Chemical Physics, 1995, 102, 2315-2325.	3.0	132
230	Quantum calculations of reaction probabilities for HO + CO→ H + CO2 and bound states of HOCO. Journal of Chemical Physics, 1995, 103, 6512-6519.	3.0	107
231	Noiseâ€free spectrum for timeâ€dependent calculation of eigenenergies. Journal of Chemical Physics, 1995, 103, 1491-1497.	3.0	13
232	Vibrational predissociation of HF dimer in $\hat{l}_{2}$ HF=1: Influence of initially excited intermolecular vibrations on the fragmentation dynamics. Journal of Chemical Physics, 1995, 102, 4382-4389.	3.0	25
233	A timeâ€dependent approach to flux calculation in molecular photofragmentation: Vibrational predissociation of HF–DF. Journal of Chemical Physics, 1995, 102, 124-132.	3.0	55
234	Fullâ€dimensional timeâ€dependent treatment for diatom–diatom reactions: The H2+OH reaction. Journal of Chemical Physics, 1994, 101, 1146-1156.	3.0	422

#	Article	IF	CITATIONS
235	Symmetry and rotational orientation effects in dissociative adsorption of diatomic molecules on metals: H2 and HD on Cu(111). Journal of Chemical Physics, 1994, 101, 1555-1563.	3.0	64
236	Quantum dynamical studies for photodissociation of H2O2 at 248 and 266 nm. Journal of Chemical Physics, 1994, 100, 5631-5638.	3.0	27
237	Quantum reactive scattering with a deep well: Timeâ€dependent calculation for H+O2reaction and bound state characterization for HO2. Journal of Chemical Physics, 1994, 101, 3671-3678.	3.0	265
238	Accurate quantum calculations for H2+OH→H2O+H: Reaction probabilities, cross sections, and rate constants. Journal of Chemical Physics, 1994, 100, 2697-2706.	3.0	120
239	Quantum mechanical calculation for photodissociation of hydrogen peroxide. Journal of Chemical Physics, 1993, 98, 6276-6283.	3.0	35
240	Total and partial decay widths in vibrational predissociation of HF dimer. Journal of Chemical Physics, 1993, 98, 5978-5981.	3.0	23
241	Accurate quantum calculation for the benchmark reaction H2+OH→H2O +H in fiveâ€dimensional space: Reaction probabilities for J=0. Journal of Chemical Physics, 1993, 99, 5615-5618.	3.0	175
242	Quantum dynamics studies of adsorption and desorption of hydrogen at a Cu(111) surface. Journal of Chemical Physics, 1993, 99, 1373-1381.	3.0	51
243	Photofragmentation of HF dimer: Quantum dynamics studies on ab initio potential energy surfaces. Journal of Chemical Physics, 1993, 99, 6624-6633.	3.0	64
244	An algebraic variational approach to dissociative adsorption of a diatomic molecule on a smooth metal surface. Journal of Chemical Physics, 1992, 97, 6784-6791.	3.0	26
245	Dissociative chemisorption of H2 on Ni surface: Timeâ€dependent quantum dynamics calculation and comparison with experiment. Journal of Chemical Physics, 1992, 96, 3866-3874.	3.0	49
246	Theoretical model for the dynamics of hydrogen recombination on the Si(100)â€(2×1) surface. Journal of Chemical Physics, 1992, 97, 596-604.	3.0	22
247	A timeâ€dependent golden rule wave packet calculation for vibrational predissociation of D2HF. Journal of Chemical Physics, 1992, 97, 927-934.	3.0	40
248	A stochastic goldenâ€rule treatment for thermal desorption of gases from solid surfaces. Journal of Chemical Physics, 1992, 96, 4729-4734.	3.0	6
249	A timeâ€dependent calculation for vibrational predissociation of H2HF. Journal of Chemical Physics, 1992, 97, 3149-3156.	3.0	34
250	QUANTUM REACTIVE SCATTERING USING THE S-MATRIX KOHN VARIATIONAL METHOD. International Journal of Modern Physics C, 1992, 03, 1351-1364.	1.7	0
251	Timeâ€dependent treatment of vibrational predissociation within the golden rule approximation. Journal of Chemical Physics, 1991, 95, 6449-6455.	3.0	47
252	Progress of basis optimization techniques in variational calculation of quantum reactive scattering. Journal of Chemical Physics, 1991, 94, 6047-6054.	3.0	43

#	Article	IF	CITATIONS
253	A fast-slow method to treat solute dynamics in explicit solvent. Physical Chemistry Chemical Physics, 0, , .	2.8	0
254	Generating and screening <i>de novo</i> compounds against given targets using ultrafast deep learning models as core components. Briefings in Bioinformatics, 0, , .	6.5	5